Characterization of Mineral Precipitates by Electron Microscope Photographs and Electron Diffraction Patterns

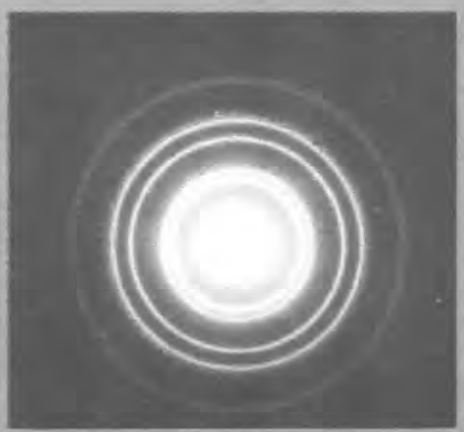

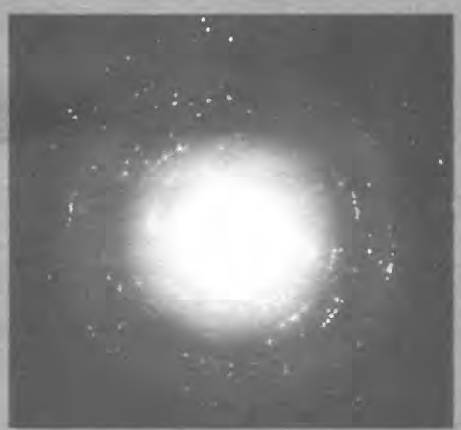

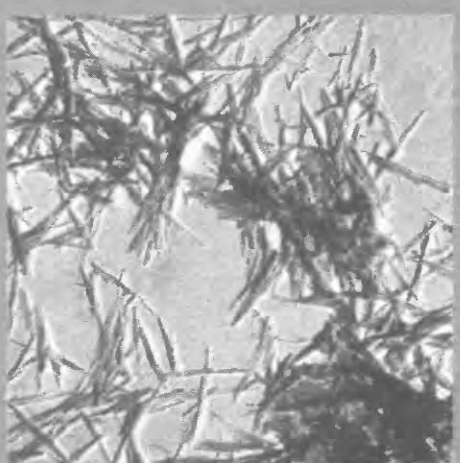

United States Geological Survey Water–Supply Paper 2204

Characterization of Mineral Precipitates by Electron Microscope Photographs and Electron Diffraction Patterns

By C. J. LIND

GEOLOGICAL SURVEY WATER-SUPPLY PAPER 2204

UNITED STATES DEPARTMENT OF THE INTERIOR
JAMES G. WATT, Secretary

GEOLOGICAL SURVEY
DALLAS L. PECK, Director

UNITED STATES GOVERNMENT PRINTING OFFICE: 1983

For sale by the Distribution Branch
U.S. Geological Survey
604 South Pickett Street
Alexandria, VA 22304

Library of Congress Cataloging in Publication Data

Lind, C. J.
Characterization of mineral precipitates by electron microscope photographs and electron diffraction patterns.

(Geological Survey Water-Supply Paper 2204)
Includes bibliographical references.
Supt. of Docs. no.: I 19.13:2204
1. Mineralogy, Determinative. 2. Electron microscopy. 3. Electron—Diffraction. I. Title.
II. Series: United States. Geological Survey. Water-Supply Paper 2204

QE369.M5L56 1983 549'.12 83-600036

CONTENTS

Abstract 1
Introduction 1
Theory 1
Electron microscope photography 1
Resolving power of the electron microscope 2
Types of electron microscopes 2
Electron diffraction 2
The diffraction pattern 3
Sample thickness limitations 3
Conditions required to make a pattern 4
Application of the Bragg law to interpret d_{hkl} spacings 4
Experimental procedure 4
Preparation of samples 4
Electron micrographs 4
Electron diffraction patterns 4
Sample mounting and diffraction pattern interferences 4
Sample portion making the pattern 5
Structural damage by the electron beam 5
Pattern interpretation 6
Radius measurement 6
Camera constant 7
Calculating d_{hkl} values 7
X-ray diffraction data 8
Results 8
Correlation of electron microscope studies, X-ray data, and published results 8
Effects of aging on manganese oxide precipitates 9
Identification of microcrystalline precipitates 9
Experimental limitations 10
Upper limit of d_{hkl} values 10
Time and effort required 17
Other applications 17
Conclusions 17
References 17

FIGURES

1. Schematic diagram of an electron diffraction pattern of a simple cubic crystal; electron micrograph of a spot pattern of manganese oxide and of a ring pattern of a gold standard 3
2. Electron micrograph showing sample material diffracting the beam, showing the center of beam focus and the entire sample encompassed by the surrounding material 6
3. Electron micrograph showing sample material damaged by beam exposure 6

4–11. Electron micrographs of identified manganese oxide precipitates:
4. γ-MnOOH, aged 20 days 8
5. Mn_3O_4, aged 1 hour 8
6. Mn_3O_4, aged 90 days; γ-MnOOH coated by Mn_3O_4 and Mn_3O_4 at a higher magnification 11
7. Poorly defined, microcrystalline manganese oxide, aged 3 hours 11
8. β-MnOOH, aged 3 days 11
9. γ-MnO_2 and Mn_2O_3, aged 66 days 13
10. β-MnOOH, aged 24 days 13
11. β-MnOOH, aged 5 months 17

TABLES

1. Electron beam wavelength, λ, as a function of the accelerating voltage, ϕ, applied to the electron gun 2
2. Calculation of the camera constant using gold as a standard 7
3–7. Correlation of electron diffraction and X-ray diffraction d_{hkl} values with published d_{hkl} values for γ-MnOOH
3. γ-MnOOH, aged 5 days and 20 days 9
4. Mn_3O_4, aged 1 hour 10
5. Partially oxidized Mn_3O_4, aged 90 days 12
6. Change in crystallinity with age, aged 3 hours and 66 days, a γ-MnO_2 and Mn_2O_3 (partridgeite) mixture 14
7. Change in crystallinity with age of β-MnOOH, aged 3 days and 24 days, and another preparation, aged 5 months 16

Characterization of Mineral Precipitates by Electron Microscope Photographs and Electron Diffraction Patterns

By Carol J. Lind

Abstract

Transmission electron micrographs and electron diffraction techniques can be used to characterize microcrystalline precipitates too minute for characterization by X-ray diffraction. Included is a description of the electron microscope, explanations of sample preparation and diffraction pattern interpretation, and examples of electron micrograph and electron diffraction applications and their limitations.

The techniques, applied to preparations of manganese oxides, show the development of crystallinity and the change in crystal form with aging. γ-MnOOH and Mn_3O_4 are identified in precipitates from two preparations. Correlation of the electron micrographs and electron diffraction patterns with X-ray diffraction patterns for these precipitates demonstrates the validity of these electron microscope techniques. Micrographs and diffraction patterns illustrate, after aging the relatively pure Mn_3O_4 precipitate, the transformation of Mn_3O_4 to γ-MnOOH. In two other preparations, electron diffraction shows diffraction patterns of precipitates whose crystals are too poorly developed to give X-ray patterns. After these preparations and another preparation were aged, the interpretation of the data indicated the precipitates to be β-MnOOH and a mixture of γ-MnO_2 and possibly Mn_2O_3. These techniques were also used to identify pure iron carbonate, iron oxides, bobierite, fluorapatite, and some aluminum sulfate sediments.

For the manganese oxides discussed, measurements by electron diffraction are as reliable as those by conventional X-ray diffraction for d_{hkl} spacings of 0.49 nm or less.

INTRODUCTION

Electron microscope photographs and electron diffraction patterns are valuable tools for characterizing microcrystalline materials and other solids whose crystallinity is not readily identifiable. The use of transmission electron microscope to obtain electron micrographs and electron diffraction techniques is described. Several microcrystalline manganese oxides are characterized in terms of crystal structure and *d*-spacings by the application of electron micrographs and electron diffraction techniques.

Microcrystalline particulates, such as clay minerals and oxides of manganese and iron, have large surface areas per unit weight and have sites for surface-mediated processes in natural water systems. The mineralogical identities and the relative concentrations of the components in microcrystalline particulates determine their cation exchange and adsorption properties and their solubility relationship controls. Also the particle size, the degree of crystallinity, and particularly, the surface composition and morphology are integral parts of the influences on these properties and controls. Consequently, meaningful and accurate water-system modeling requires characterization of microcrystalline particulates.

Chemical analysis, surface area determination, and X-ray diffraction are common means used to characterize these particulates. However, particulates that are still in the initial stage of formation, those that are in transition from one mineralogical form to another, or those that are in their last stages of dissolution can be too minute to permit mineralogical identification by X-ray methods.

X-ray patterns of well-crystallized, larger than 0.1 μm, material with no lattice strains show reasonably sharp X-ray diffraction lines at all angles. As the particle size decreases below 0.1 μm, the X-ray diffraction lines become less sharp and patterns of crystallites smaller than 0.01 μm show no back reflection and very wide, diffuse, low-angle X-ray lines (Klug and Alexander, 1974). The manganese precipitates used here for illustrative purposes are primarily in the 0.1 μm and less size range.

THEORY

Electron microscope photography

An electron microscope is essentially an inverted optical microscope that uses electrons instead of light

and that has magnetic lenses instead of glass lenses. A negative dc-accelerating voltage applied to the tungsten cathode produces an electron beam. Under high vacuum, a focused, accelerated electron beam impinging on fluorescent screen creates a visible image.

Resolving power of the electron microscope

According to Haine and Cosslett (1961), the resolving power, the finest detail a microscope can resolve, is limited by the relationship:

$$d = 0.61\lambda/\sin\alpha, \quad (1)$$

where d is the radius of the radiation patch that images an infinitely small radiating object, λ is the wavelength of illumination, and α, the angular aperture, is the semiangle of the light cone leaving a point in the object and entering the objective lens. The collection of all possible illuminating radiation, as required by high magnifications, is facilitated by a large angular aperture. Thus, the best resolution is given by large α values and short λ. The upper limiting value for $\sin\alpha$ is 1, hence d is effectively limited to a value near 0.61λ.

The unaided eye can perceive detail no finer than about 0.1 mm. The resolving power of a light microscope is limited to values near the green light wavelength, about 500 nm. The electron beam wavelength is up to 10^{-5} times the wavelength of visible light, and thus the electron microscope has potential for a much greater resolving power.

Haine and Cosslett (1961) derived the term:

$$\lambda = \sqrt{(1.5/\phi)}\ \text{nm}, \quad (2)$$

where ϕ is the applied accelerating voltage. The value 100 kV (the accelerating voltage used in this work) applied to equation 2 gives a λ of 0.0037 nm. This value, smaller than the interatomic spacings in a solid, suggests the possible magnitude of electron microscope magnification. Electron diffraction patterns, described later, are an illustration of the passage of electrons between atoms in a solid. (Table 1 lists the values of λ for potentials ranging from 20 kV to 4000 kV.)

The detail and contrast in the sample limit the usable degree of resolution. A thin metal coating applied to the test material by a sample-coating device improves the contrast. The metal coating, applied at a selected angle, creates a shadowing effect and makes possible an estimate of particle thickness.

Types of electron microscopes

There are two general types of electron microscopes, the scanning electron microscope and the transmission electron microscope. Just as the eye views a three-dimensional surface by light reflected from an object, the scanning electron microscope images a three-dimensional surface by electrons reflected from a sample. The transmission electron microscope images outlines of both thick and thin samples by the electrons passing by the sample and images structural features of thin samples by electrons passing through the samples.

Table 1.—*Electron beam wavelength, λ, as a function of the accelerating voltage, ϕ, applied to the electron gun*

[After Beeston and others, (1972)]

Accelerating Voltage, ϕ (kV)	Wavelength, λ (nm)
20	0.00859
30	.00698
40	.00602
50	.00536
60	.00487
70	.00448
80	.00418
90	.00392
100	.00370
200	.00251
300	.00197
400	.00164
500	.00142
600	.00126
700	.00113
800	.00103
900	.00094
1000	.00087
2000	.00050
4000	.00028

Electron diffraction

The electron microscope produces electron diffraction patterns by diffracting a collimated electron beam projected onto a sample. In a crystalline solid, planes of atoms, lying at angles θ to the incident beam, diffract some of the beam's electrons as the electrons pass through the sample. The diffracted electron beam forms a pattern of spots, each representing an image of the beam refracted from one of the planes of atoms. The pattern is viewed as the beam impinges on a fluorescent viewing screen and is recorded as the beam strikes a photographic film or plate. Interpretation of the recorded pattern can define many of the spacings between the atomic planes (d_{hkl}'s) in the one or more substances the sample contains. From these spacings, along with supplementary information, the identities of the minerals present can be deciphered. The tendency toward a preferred orientation in the electron diffraction sample causes some d_{hkl} spacings to be missing and the spot intensities to differ from the peak intensities obtained by X-ray diffraction. Ross and Christ

(1958), Ross (1959), Andrews and others (1967), and Beeston and others (1972) describe interpretation of cell dimensions and crystal form from electron diffraction patterns.

The diffraction pattern

Particles larger than 0.1 μm produce electron diffraction spot patterns, and particles from 0.1 μm to 0.01 μm produce continuous ring electron diffraction patterns (Andrews and others, 1967). (The upper size limit for electron diffraction is discussed in the next section.) Also, a single crystal creates an ordered array of spots and several randomly oriented crystals of the same material create an arrangement of these spots in concentric rings. As the number of crystals and randomness increase, the spots merge, forming partial or complete rings. Well-defined crystals give distinct patterns. However, the minute size and poorly crystalline state of the material studied here produce faint patterns that in some cases required darkening for visibility against the measuring grid. Figure 1*A* is a schematic diagram of a spot pattern representing a simple cubic crystal structure; that is, sodium chloride. Figure 1*B* shows a spot pattern produced by several crystals that were in the electron beam path and represents a sample discussed later in this work. Figure 1*C* is a ring display produced by a film of gold plating used as a standard in this work.

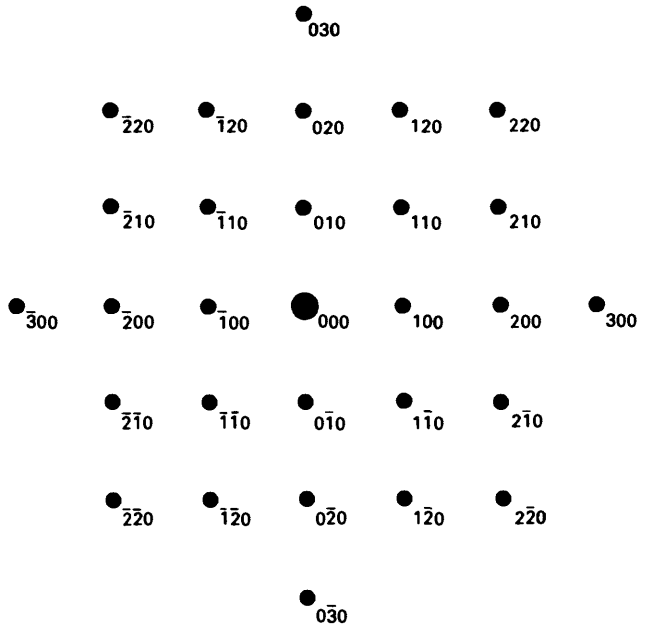

Figure 1A.—A schematic of a diffraction pattern for a simple cubic crystal. The numbers represent the Miller indices of the lattice planes from which the spots arise (from Beeston and others, 1972).

Sample thickness limitations

The rather low penetrating power of electrons restricts electron diffraction to thin, electron-transparent samples. According to Goodhew (1972), the intensity of the electrons transmitted depends on the electron scattering factor of the sample, and the scattering factor is related to the atomic number of the sample atoms. For example, at 100 kV, an amorphous aluminum sample, several tenths of a micron thick, yields a usable pattern. To obtain a pattern from a

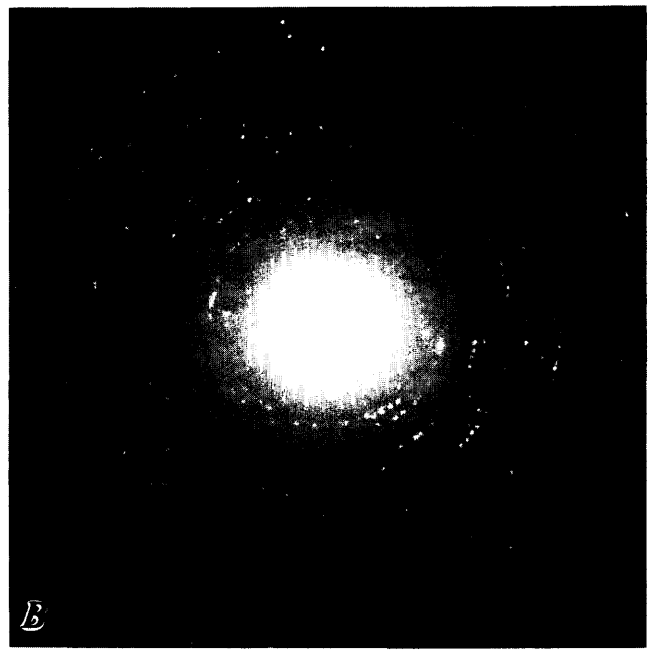

Figure 1B.—Electron diffraction spot pattern of a sample.

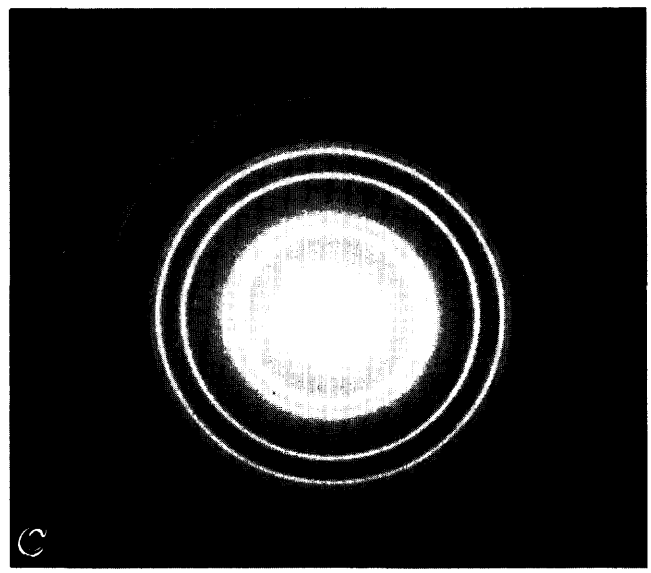

Figure 1C.—Electron diffraction ring pattern of a gold standard.

uranium sample, the sample must be near a few hundredths of a micron in thickness. Utilization of the tilt mechanism on the microscope stage allows the examination of slightly buckled samples with restricted areas of proper orientation. This mechanism permits penetration of several microns of aluminum or more than one tenth of a micron of uranium. An image intensifying device, described later in this paper, facilitates the examination of samples up to twice the normal permissible thickness. Thicker samples can be penetrated by increasing the accelerating voltage. Voltages in the MeV range have been used (Goodhew, 1972). Thick samples that the electrons cannot penetrate can be thinned. The sample character governs the thinning technique chosen. Goodhew (1972) described sample-thinning techniques in detail.

Conditions required to make a pattern

Discrete diffraction spots occur only for conditions satisfying the Bragg law. The Bragg law is

$$\lambda = 2d_{hkl} \sin \theta \quad (3)$$

where λ is the incident electron beam wavelength, d_{hkl} is the spacing between the individual planes, and θ is the diffraction angle. As already stated, the wavelength varies with the accelerating voltage applied to the electron gun.

Application of the Bragg law to interpret d_{hkl} spacings

Bragg's law can be simplified to a useful approximation. By simple geometry

$$\tan 2\theta = R/L \quad (4)$$

where R is the distance from the diffraction-pattern center to the spot or ring in question and L, the camera length, is the distance between the specimen and the photographic plate or film. (Actually, the "effective camera length" varies with the instrument settings.) Because the angles θ through which the electrons are diffracted are very small (only $1° - 2°$), there is little error in the approximation

$$\tan 2\theta = 2\sin \theta. \quad (5)$$

Thus

$$R/L = \lambda/d_{hkl} \quad (6)$$

which rearranges to

$$d_{hkl} = \lambda L/R. \quad (7)$$

Adjustments to the high-voltage supply, adjustments to the lens currents, instabilities in the electron circuitry, or utilization of the specimen-tilting mechanism can alter the term, λL (the camera constant). Thus, the camera constant must be determined for each set of diffraction patterns (Beeston and others, 1972). Once the camera constant is determined, the d_{hkl} spacings of the sample can be calculated. The distance of each spot or ring from the central spot of the sample pattern is measured, and this value is inserted in equation 7 along with the established camera constant, giving the d_{hkl} represented by that spot or ring.

EXPERIMENTAL PROCEDURE

The instrument used in this study for both electron micrographs and electron diffraction patterns is an A.E.I. transmission electron microscope, model EM6G[1], which has a 30–100-kV range and a 600–120,000-magnification range.

Preparation of samples

Residues, obtained by filtering suspensions of solids, were resuspended while still damp and then dispersed in an ultrasonic bath. Drops of this suspended sample were dried successively on Formvar-covered copper grids of 200 or 300 mesh. Using a Thermionic diffusion pump evaporator, model TL1–10, the dried sample was then coated with platinum metal directed at an angle of 45°. Kay (1965) and Goodhew (1972) present detailed descriptions of various mountings methods for many kinds of samples.

Electron micrographs

A series of micrographs for each sample was made to illustrate sample crystallinity. Each sample photographic series includes several degrees of magnification for several sample areas and from mounts on more than one grid. Depending on the discernible sample detail, the magnification is from 10,000 to 100,000. Depending on the resolution shown on the negatives, the final photographic prints were enlarged by two, three, or four times, and they range in magnification from 20,000 to 320,000.

Electron diffraction patterns

Sample mounting and diffraction pattern interferences

The samples for electron diffraction must be mounted differently than those for electron micrographs. The platinum coating on the samples prepared for electron micrographs masks the sample pattern with a platinum pattern. Copper diffraction patterns of

[1]Mention of brand names is for identification only and does not imply endorsement by the U.S. Geological Survey.

the copper grids can adulterate diffraction patterns of samples.

For diffraction patterns, only one drop of suspended sample is dried on carbon-coated Formvar films mounted on MaXtaform H5 grids. The use of only one drop minimizes the opportunity for grid corrosion caused by successive applications and evaporations of suspensions. The carbon support films give greater mechanical strength and stability under electron bombardment. The hexagonal holes of the MaXtaform H5 grids retain the necessary film support and the resulting increased hole area permits sample examination away from grid-metal interference.

The examination of five sample areas and at least two sample mountings gives a representation of the test material discussed here. The examination of the sample mounted on two or more grids, one gold and the other nickel or copper-rhodium, helps to distinguish the sample pattern from a possible grid-metal pattern.

Sample portion making the pattern

The diameter of an aperature opening controls the size of the area of the sample diffracting the beam. Decreasing the opening decreases the area. Beeston and others (1972) recommend 1μm as the lower limit for the diameter of the sample area subjected to the electron beam. When using a modern high-resolution microscope set at 100 kV to examine a 1 μm diameter area, they calculated that the size and location of the area of the sample is subject to a typical 24 percent uncertainty due to spherical aberrations. The 24 percent is for low-order reflections. A high-voltage electron microscope set at 1,000 kV gives this 24 percent accuracy for 15 nm diameter area. Also, frequently occurring image focusing inaccuracies, such as with a thick sample, cause further inaccuracy of area selection. The combined effect is that, for a setting of 100 kV, an area of less than 1 μm in diameter cannot be selected with any reasonable accuracy (or, for a setting of 1,000 kV and a similar degree of focusing inaccuracy, an area possibly of less than 0.1 μm).

The sample area examined by electron diffraction is very small compared to that examined by X-ray diffraction in a smear or power pack. In addition, electron diffraction is capable of characterizing a very select sample portion. If only small amounts of sample are available or if individual sample components are examined, the electron diffraction method may be the most satisfactory procedure. Characterization of individual sample components by electron diffraction requires that the components be well separated on the sample mount. The separation must be such that only the component to be examined is in the vicinity of the area to be viewed. However, as will be shown later in this paper, the characterization of sample components with more than one component in the viewing area is possible when sufficient supporting information is available.

In the present experiments the sample portion diffracting the beam is approximately 6 μm in diameter. Two photographs of the diffracting material are made after each diffraction pattern is photographed. The 50,000 magnification exposure, figure 2*A*, indicates the detailed sample morphology. This exposure is a view of sample material located at the center of the diffraction beam. The 8,000 magnification photo, figure 2*B*, shows the entire sample that is diffracting the beam. The 8,000-magnification photograph is exposed twice on the same negative, once with only the diffracting material and then again with both the diffracting material and the surrounding material. Figures 2*A* and 2*B* correspond to the diffraction pattern shown in figure 1*B* and are identified in table 5 as Mn_3O_4 + γ-MnOOH.

Structural damage by the electron beam

A strong electron beam can damage or destroy the sample structure and sometimes even change the sample composition or completely evaporate the sample. When viewed as an electron micrograph, a beam-damaged sample may show indistinct details and appear out of focus, the sample may appear partly melted, or the sample may just disappear by bubbling and boiling away as it is being viewed. Figure 3 illustrates the fuzzy, melted appearance of a beam-damaged sample. Beam damage may change a diffraction pattern to a different array of spots or rings or may weaken or completely obliterate the pattern. Beam damage is minimized by focusing with as low an electron beam intensity as practical. Photographing the diffraction pattern before photographing the 50,000- and 8,000-magnification electron micrographs records the pattern with a minimum of sample structure alteration. Beam damage and lack of shadowing may cause the above micrographs to show less detail than the micrographs of the platinum-coated sample. Thus, the platinum-coated samples are generally better for examination of overall sample morphology.

An image-brightener attachment permits examination with a low-beam intensity and viewing of patterns that otherwise would be difficult or impossible to see on the fluorescent screen. As mentioned earlier, this attachment also makes it possible to get diffraction patterns of thick samples.

Figure 2.—Electronmicrographs of sample material diffracting the beam (pattern of sample is shown in fig. 1*B*). *A*, The view at the center of beam focus. (Film view is 50,000 magnification.) *B*, View of the entire sample portion producing the diffraction pattern (lighter background) and the surrounding material (darker background). (Film view is 8,000 magnification.)

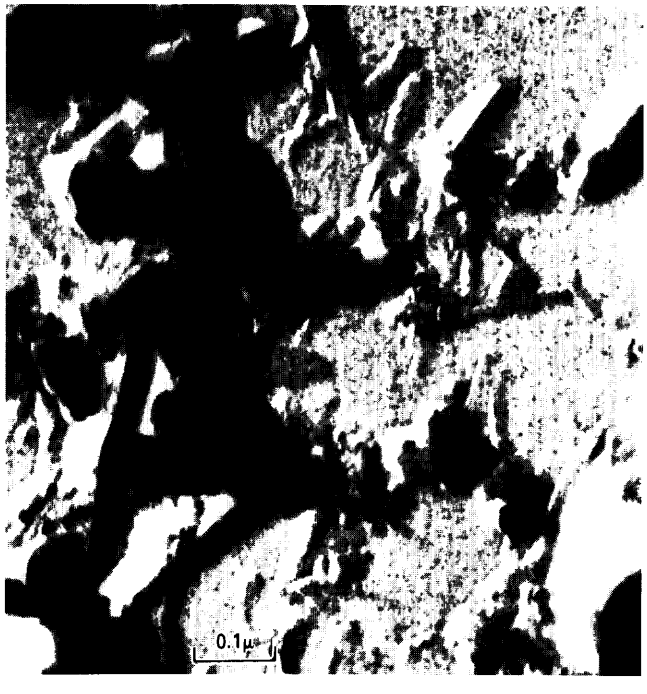

Figure 3.—Sample material that has suffered structural damage from beam exposure. The dark wide border around the darker sample material and poor definition of some of the pale material is caused by beam damage.

Pattern interpretation

Radius measurement

The radii of the diffraction patterns are measured by placing the film image over a fine-lined measuring grid on a light table. The pattern is viewed through a magnifying lens, and the less distinct spots and faint rings are marked with a fine-tipped pen to make them more visible against the grid. Another mode of measuring the radii is with a measuring microscope.

Accurate measurement of diffraction-ring radii requires meticulous care. The procedure is even more tedious when detailed spot patterns rather than rings are present. Generally the radius of a ring can be closely ascertained by measuring the diameter. As opposed to measuring radii directly, measuring the diameter and then calculating R increases the final d_{hkl} accuracy. To measure R for a pattern of spots, the center of the pattern is located as precisely as possible, then the distance from the center to each spot is measured. Operator judgment is required to ascertain the significance of radius mesurements observed for only one spot, or for only a few spots and for measurements that are nearly but not exactly equal. Figure 1*B* illustrates detailed spot patterns. For many of the samples, an estimate of the relative intensity of a spot or ring

and (or) of the relative frequency of each R occurrence are listed in the tables of d_{hkl} spacings. (Within the limits of measurement precision, the averaged R accuracy increases with the frequency of occurrence.)

Determination of d_{hkl} values can be facilitated by means of a diffraction pattern measuring device with a densitometer and chart recorder. The apparatus automatically produces a permanent expanded chart record of film density variations along the selected scanning track. The pattern can be read to between 0.05 and 0.1 mm count of the line spacing for d_{hkl} value determinations, depending on the chart speed and the scanning speed choice. Extremely weak lines, line segments, and spots can be evaluated. This increased radii-measurement capacity extends the usefulness of the electron diffraction pattern and improves measurement precision.

Camera constant

Several methods of determining the camera constant were discussed by Hall (1966), Andrews and others (1967), Rymer (1970), and Beeston and others (1972). One method is to apply equation 7 to values derived from a ring pattern of a standard material such as gold. The metal is plated onto a small part of the sample grid, and a ring diffraction pattern is photographed on an area where there is no sample material. Using the same grid for standard and sample patterns minimizes the need to alter the camera settings between those used for the standard and those used for the sample unknown. The constant is obtained as follows: (1) the diameter of each of the sharp, complete rings on the gold standard diffraction pattern is measured; (2) each of these diameters is halved and then multiplied by its associated gold d_{hkl} value; (3) these products are averaged. The average is considered the camera constant.

The camera constant might be better named the diffraction pattern constant as it is specific for each set of patterns and for each direction the radius is measured. For this work, the constant was determined for measurements across the film and for measurements lengthwise of the film. Although the camera constants were determined with each set of diffraction patterns with the microscope left on and the settings not greatly altered, the camera constants for the two directions varied from pattern set to pattern set by about ±0.5 percent or less over a period of a day. Changes in instrument settings and in precision of pattern measurement contribute to the apparent variance.

Figure 1*C* shows a gold standard pattern and table 2 illustrates the calculation of the two averaged camera constants.

Calculating d_{hkl} values

The camera constant and each measured value for R applied to equation 7 give a sample d_{hkl} value. The camera constant chosen is the one corresponding most closely to the direction of the particular test sample R measurement. Because ring patterns represent a type of averaged spot pattern, their R's are measured and their d_{hkl} values are calculated for the two directions of camera constant determination, and then the results are averaged. All the d_{hkl} values obtained for the manganese samples are summarized (tables 3 through 7). Because of their questionable reliability, d_{hkl} values that occur only once or twice are not part of the initial correlation of electron diffraction d_{hkl} values

Table 2.—*Calculation of the camera constant using gold as a standard*

Gold literature values[1] *A.S.T.M. Index no. 4–784*		*Calculations lengthwise of film*		*Calculations across film*	
hkl	d_{hkl}	*Measured Camera constant*		*Measured Camera constant*	
		radius	(d_{hkl} × *Radius*)	*radius*	(d_{hkl} × *Radius*)
	(nm)	*(mm)*	*(μm²)*	*(mm)*	*(μm²)*
111	0.2355	6.86	1.616	7.04	1.658
200	.2039	7.98	1.627	8.09	1.650
220	.1442	11.24	1.621	11.45	1.651
311	.1230	13.16	1.606	13.41	1.649
222	.1177	13.76	1.620	14.07	1.656
331	.09358	17.36	1.625	17.68	1.654
420	.09120	17.82	1.625	18.20	1.660
422	.08325	19.53	1.626	19.92	1.658
Average			1.621	----	1.654

[1]Taken from Smith and others (1960).

with reported d_{hkl} values. These questionable values are added later to further confirm the sample identity. Groupings of d_{hkl} values that vary within measurement error are averaged to give the reported d_{hkl} value.

X-ray diffraction data

The X-ray diffraction data were obtained with a Phillips X-ray diffractometer. The samples were mounted either by drying the precipitate directly on a glass slide or by cementing the sample-coated Millipore or Nuclepore polycarbonate filter membrane onto the slide. A thin dried sample layer on the filter membrane usually cannot be removed. The Nuclepore membrane itself gives a broad peak at about 0.506 nm, so sample peaks with a d_{hkl} value near this dimension must be pronounced enough to be distinguished from the Nuclepore peak. The results reported here note which samples were mounted on Nuclepore membranes.

RESULTS

Experimental data that characterize some synthetic manganese oxides demonstrate the usefulness of electron microscopy. The oxides were prepared by aeration of manganous perchlorate and manganous sulfate solutions at pH's between 8.5 and 9.5 and at temperatures between 0° and 25°C; they were aged in solution. The nature of these oxides is difficult to determine exactly. They tend to be complicated mixtures of Mn^{2+}, Mn^{3+}, and Mn^{4+} species; the crystals are very small and often poorly developed. (The test materials were prepared as part of a study of these oxides by J. D. Hem and C. E. Roberson. The oxide preparation details will be described in later publication(s) of the study results.

The experimental data shown here illustrate the applicability of electron microscope photographs and of electron diffraction to the interpretation of microcrystalline morphology. The micrographs give a direct view of the morphology of microcrystalline samples. Also the degree of crystallinity indicated by the photographs helps to predict the quality, type, and detail of the diffraction patterns. Electron diffraction is particularly helpful for the determination of d_{hkl} spacings in very small crystals.

Correlation of electron microscope studies, X-ray data, and published results

Tables 3 and 4 show evidence that d_{hkl} spacings from electron diffraction patterns for known materials correlate with results obtained by previous workers as well as or better than spacings determined by X-ray diffraction. The data in tables 3 and 4 indicate conclusively that the test samples are γ-MnOOH and Mn_3O_4

Figure 4.—View of platinum-shadowed, needle-shaped γ-MnOOH crystals, aged 20 days, showing their tendency to clump together into balls.

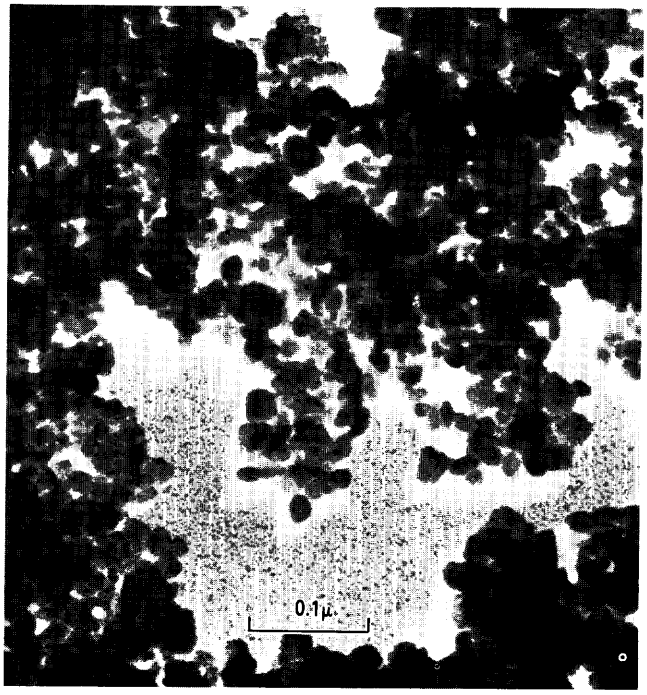

Figure 5.—View of platinum-shadowed, pseudocubic Mn_3O_4 crystals, aged 1 hour.

Table 3.—*Correlation of electron diffraction and X-ray diffraction d_{hkl} values with published d_{hkl} values for γ-MnOOH*

[Intensities listed relate to largest peak numerically or in terms of W (weak), S (strong), V (very), and M (medium)]

This work						Literature data[1]	
Age, 5 days		Age, 20 days					
X-ray diffraction		Electron diffraction		X-ray diffraction		X-ray diffraction	
d_{hkl} (nm)	I	d_{hkl} (nm)	I	d_{hkl} (nm)	I	d_{hkl} (nm)	I
0.413	B[2]	(0.414	W)[3]	----	----	----	----
.338	10	(.344	S)	0.338	10	0.341	10
.263	5	(.270 –	VW)[4]	.263	4	.265	5
----	----	(.257	VW)	.252	1	.252	1
----	----	.243	S	.240	4	.241	8
.226	3	.223	M	.226	3	.228	3
----	----	----	----	.220	2	.220	3
.1767	1	(.179	M)	.1773	2	.1781	2
.1703–?	B[2]	----	----	.170–?	B[2]	.1710	.5
.1674	B[2]	(.168	S)	.167	5	.1675	9
----	----	----	----	----	----	.1637	.1
----	----	(.1567	VS)	----	----	----	----
.150	B1[2]	(.150	W)	.150	2	.1502	.1
.1434	B1[2]	.1437	VS	.1433	2	.1435	1.5
----	----	.1331	M	.133	1	.1323	.5
----	----	.1274	M	.1318	1	.1262	.2
----	----	.1225	M	----	----	.1214	.2
----	----	----	----	----	----	.1182	.1
----	----	(.1153 –	VW)	----	----	.1158	.1
----	----	----	----	----	----	.1139	.2
----	----	----	----	----	----	.1118	.1
----	----	(.1106	VW)	----	----	.1089	.2
----	----	(.1081 –	VW)	----	----	.1080	.1
----	----	(.1016 –	M)	----	----	.1015	.1
----	----	.0989	S	----	----	.0993	.1
----	----	.0938	M	----	----	----	----
----	----	(.0905 –	S)	----	----	----	----
----	----	.0900	M	----	----	----	----

[1]Taken from Bricker (1965).
[2]B broad peak.
[3]( ) found on only one grid.
[4](–) found in only one view.

respectively. Figures 4 and 5 show electron microscope views of these platinum-shadowed materials.

Effects of aging on manganese oxide precipitates

The usual precipitate obtained by aerating dilute manganous perchlorate solutions at a pH of 8.5 to 9.5 is Mn_3O_4, hausmannite (Hem, 1980). The material shown in figure 5 is Mn_3O_4 that was precipitated in this way at pH 8.5 and 27°C. The suspension was sampled immediately after completion of the reaction; the precipitate consisted of masses of individual crystals a few hundredths of a micron in diameter. The suspension was aged in a covered beaker for 3 months and then resampled. During this period the precipitate was partly altered to γ-MnOOH, the long needles of which can be seen in figures 6*A* and 6*B*.

Electron and X-ray diffraction data for the freshly prepared and the aged samples are given in tables 4 and 5.

Identification of microcrystalline precipitates

Poorly crystallized microcrystalline materials from two different preparations are shown in the micrographs; they are so undeveloped that they give little or no X-ray patterns. In spite of their poorly developed

Table 4.—*Correlations of electron diffraction and X-ray diffraction d_{hkl} values of freshly prepared samples (age 1 hour) with published d_{hkl} values for Mn_3O_4*

[Electron diffraction values from ring patterns. Intensities listed numerically relative to largest peak or in terms of W (weak), S (strong), V (very), and M (medium)]

This work				Literature data[1]	
Electron diffraction		X-ray diffraction		X-ray diffraction	
d_{hkl} (nm)	I	d_{hkl} (nm)	I	d_{hkl} (nm)	I
0.493	W	?-nuclepore peak		0.492	8
.312	M	0.309	2	.308	8
----	----	.287	1	.287	2
.279	M	.276	5	.276	9
.250	VS	.247	10	.248	10
----	----	.234	1	.236	4
.2049	S	.203	2	.203	6
.1817	M	----	----	.1828	5
----	----	.176	2	.1795	4
.1715	W	.170	1	.1700	2
----	----	.164	1	.1641	2
.1562	VS	.158	4	.1575	4
----	----	.154	6	.1542	9
.1448	S	.144	3	.144	3
----	----	----	----	.1381	1
----	----	----	----	.1346	2
.1287	M	.127	1	.1277	3
.1233	M	----	----	.1229	2
.1191	M			.1193	2
.1132	M			.1122	1
.1080	M			.1081	2
----	----			.1061	1
----	----			.1030	2
.1025	M			.1019	2
.09823	M			.0985	2

[1]Taken from Bricker (1965).

crystallinity, they give definable electron diffraction patterns that show γ-MnO_2, nsutite, age 3 hours, and β-MnOOH, age 3 days, might be forming (figs. 7 and 8 and tables 6 and 7, respectively).

Evidence of the crystal structures being formed is shown further for γ-MnO_2 and possibly for Mn_2O_3 at age 66 days. The diffraction data for this aged material corresponds with the literature data for γ-MnO_2 (nsutite), Mn_2O_3 (partridgeite), and MnO_2 (ramsdellite). γ-MnO_2 may have ramsdellite and pyrolusite intergrowths (Burns and Burns, 1977). Faulring (1965) describes nsutite as hexagonal in form; Bricker (1965) describes nsutite as lathlike in appearance. According to Bystrom (1949) and Swanson and others (1974), ramsdellite and partridgeite both may be orthorhombic. In light of the above, the micrographs show the crystal forms to be expected (table 6 and fig. 9).

Compared to the poorly defined preparation at age 3 days, this same preparation at 24 days and another preparation at 5 months gave much better evidence of β-MnOOH formation. Bricker (1965) describes β-MnOOH as hexagonal- and lath-shaped platelets. Both the micrographs and the diffraction data agree with the literature data as to the formation of β-MnOOH (table 7 and figs. 10 and 11).

Experimental limitations

Upper limit of d_{hkl} values

According to Beeston and others (1972), unless the measured value of R (the radius of a diffraction ring or the distance from a spot to the center of the ring) is 4 mm or more, the accuracy of the d_{hkl} will not be satisfactory. Spots closer to the center tend to become lost in the diffuse scattering of electrons around the central spot. This phenomenon sets an upper limit of d_{hkl} values that can be measured reliably by electron diffraction.

Photographs of diffraction patterns for a gold standard were made before and after the test sample patterns were photographed. The camera constant values from 15 of these gold diffraction patterns (all taken at 100 kV) were averaged and applied to equation 7. Using the recommended 4-mm distance for measurements of R, the maximum d_{hkl} is 0.405 nm for measurements lengthwise of the film and 0.426 nm for measurements across the film. Assuming a decrease in voltage from 100 to 80 kV changes the camera constant by only the amount caused by the λ increase listed in table 1, the maximum d_{hkl} values that can be measured at 80 kV using the recommended 4-mm minimum distance are 0.458 nm and 0.467 nm, respectively. Beeston and others (1972) did not recommend voltages lower than 80 kV because of decreased specimen penetration and increased chromatic blurring of the image.

Figure 6.—View of platinum-shadowed, partially oxidized Mn_3O_4. *A*, Mn_3O_4 crystals coating γ-MnOOH needles, aged 90 days, and *B*, same material but at four times the magnification of view *A*, making the crystal shape of Mn_3O_4 more obvious.

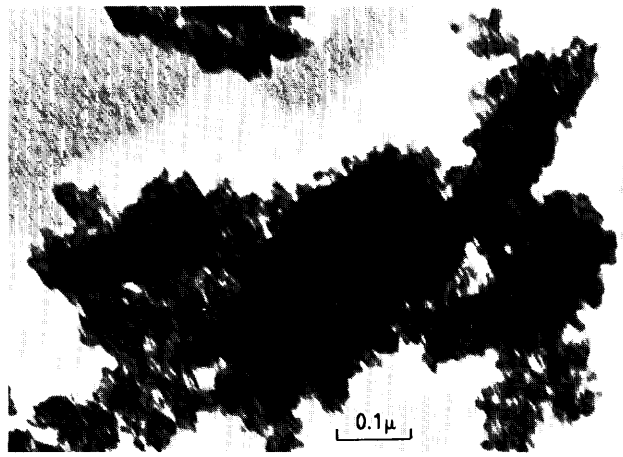

Figure 7.—View of platinum-shadowed, poorly defined, microcrystalline manganese oxide, aged 3 hours.

Figure 8.—View of platinum-shadowed, poorly defined, microcrystalline β-MnOOH from preparation 1, aged 3 days.

Table 5.—*Correlation of electron diffraction and X-ray diffraction d_{hkl} values of aged, partially oxidized Mn_3O_4 samples with published d_{hkl} values*

[For electron diffraction, four grids were examined and because there were so many spots, only the spots adjacent to the two axes for the camera constant determination were considered. For electron diffraction, intensities are listed numerically relative to the most number of spots measured with a specific d_{hkl} and for X-ray diffraction, intensities are listed numerically relative to the largest peak]

This work				*Literature data*			
Partially oxidized Mn_3O_4 Age, 90 days				[1]*Mn_3O_4*		[2]*γ-MnOOH*	
Electron diffraction		*X-ray diffraction*		*X-ray diffraction*		*X-ray diffraction*	
d_{hkl} (nm)	*I*	d_{hkl} (nm)	*I*	d_{hkl} (nm)	*I*	d_{hkl} (nm)	*I*
----	----	?-nuclepore		----	----	----	----
----	----	peak	0.08	----	----	----	----
----	----	0.493	----	0.492	8	----	----
[3](0.342 –	2)	.340	10	----	----	0.340	10
----	----	.308	.09	.308	8	----	----
(.295 –	0.7)	.288	.05	.287	2	----	----
.275	2	.276	.2	.276	9	----	----
.264	9	.264	2	----	----	.264	5
.256	6	----	----	----	----	----	----
.253	7	----	----	----	----	.253	3
.249	2	.248	.3	.248	10	----	----
(.246 –	.2)	----	----	----	----	----	----
.244	3	----	----	----	----	----	----
(.242 –	2)	----	----	----	----	.242	7
[4](.238	1)	----	----	----	----	----	----
(.236	.7)	.236	.07	.236	4	----	----
.229	4	.227	1	----	----	.228	4
.224	1	.223	.2	----	----	----	----
.221	5	----	----	----	----	.220	4
.216	3	----	----	----	----	----	----
.202	3	.204	.08	.203	6	----	----
.183	4	----	----	.1828	5	----	----
.181	3	----	----	----	----	----	----
.180	7	.179	.07	.1795	4	.179	6
.172	4	.170	2	.1700	2	.171	4
.167	3	.167	.1	----	----	----	----
.164	5	.163	.8	.1641	2	.164	8
.161	2	----	----	----	----	----	----
.159	3	----	----	----	----	----	----
(.157 –	1)	----	----	.1575	4	----	----
----	----	.155	.09	----	----	----	----
.154	5	.154	2	.1542	9	----	----
.152	4	----	----	----	----	----	----
.150	6	----	----	----	----	.150	4
.147	7	----	----	----	----	----	----
.144	10	----	----	.144	3	.144	4
.142	7	.143	2	----	----	.143	4
.140	5	----	----	----	----	----	----
.139	4	----	----	.138	1	----	----
.136	6	----	----	.1346	2	----	----
.132	8	.1323	.2	----	----	.132	4
.130	3	.1296	6	----	----	.130	1
.128	5	----	----	.1277	3	.128	1
.126	5	----	----	----	----	.126	2
.124	7	----	----	.1229	3	.124	1
(.122	1)	----	----	----	----	.121	2

Table 5.—*Correlation of electron diffraction and X-ray diffraction d_{hkl} values of aged, partially oxidized Mn_3O_4 samples with published d_{hkl} values—Continued.*

This work				Literature data			
Partially oxidized Mn_3O_4 Age, 90 days				[1]Mn_3O_4		[2]γ-MnOOH	
Electron diffraction		X-ray diffraction		X-ray diffraction		X-ray diffraction	
d_{hkl} (nm)	I	d_{hkl} (nm)	I	d_{hkl} (nm)	I	d_{hkl} (nm)	I
.120	5	----	----	.1193	2	----	----
.117	6	.1181	.06	.1180	2	.118	4
(.115 –	1)	----	----	----	----	.116	3
.113	5	.1137	.7	----	----	.113	4
.111	4	.1116	.2	----	----	.111	3
----	----	----	----	.1099	1	.109	3
.108	1	----	----	.1081	2	.108	3
(.105 –	.8)	----	----	.1061	1	----	----
.103	2	----	----	.103	2	.103	4
----	----	----	----	.1019	2	.102	2
.100	3	----	----	----	----	.101	4
(.0986	4)	----	----	.0985	2	.099	4

[1]Taken from Bricker (1965).
[2]Taken from Gattow (1962).
[3](–) found in only one view.
[4]( ) found on only one grid.

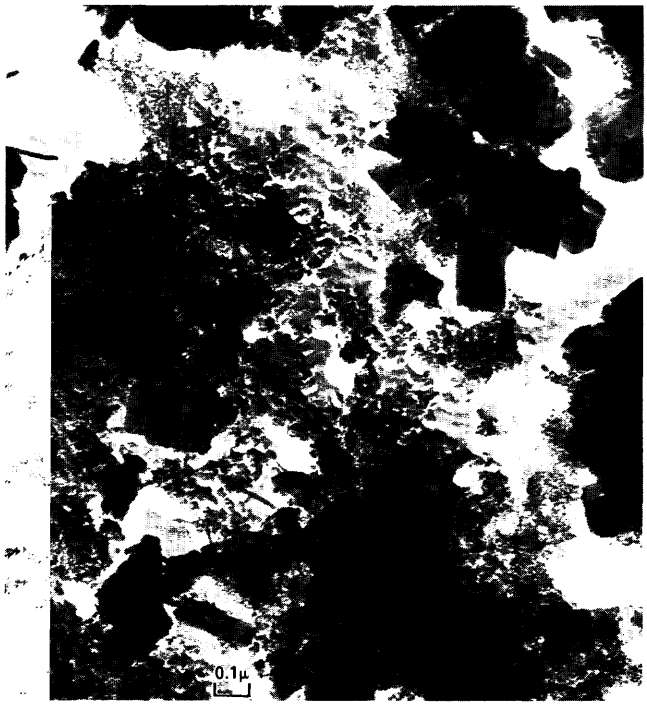

Figure 9.—View of platinum-shadowed precipitate of manganese oxide from the same preparation as shown in figure 7. Here the preparation has been aged 66 days and definite crystal shapes can be seen. This view is 0.4 times the magnification of the view shown in figure 7.

Figure 10.—View of platinum-shadowed, hexagonal- and lath-shaped platelets of β-MnOOH from preparation 1, aged 24 days. This view is at twice the magnification of the view of the 3-day-old material shown in figure 8.

Table 6.—*Change in crystallinity with age and the correlation of electron diffraction patterns and a poorly defined X-ray diffraction pattern with published d_{hkl} values for nsutite, ramsdellite, and partridgeite*

[For electron diffraction, the data for the 3-hour-old material was derived from ring patterns and the data for the 66-day-old material was derived from spot patterns. Also for electron diffraction, the number under intensity denotes the ratio of the number of rings or spots measured with that d_{hkl} to the most number of rings or spots with a specific d_{hkl}, and the actual intensities are listed in terms of W (weak), S (strong), M (medium), V (very), and tr (trace). For X-ray diffraction, the intensities are listed numerically relative to the strongest peak.]

This work								Literature data					
Age, 3 hours				Age, 66 days				[1]γ-MnO_2 Nsutite		[2]MnO_2 Ramsdellite		[3]Mn_2O_3 Partridgeite	
Electron diffraction		X-ray diffraction		Electron diffraction		X-ray diffraction		X-ray diffraction		X-ray diffraction		X-ray diffraction	
d_{hkl} (nm)	I	d_{hkl} (nm)	I	d_{hkl} (nm)	I	d_{hkl} (nm)	I	d_{hkl} (nm)	I	d_{hkl} (nm)	I	d_{hkl} (nm)	I
----	----	Showed	----	0.537	1	----	----	----	----	----	----	----	----
----	----	no	----	.472	10	----	----	----	----	0.464	2	0.4706	1
----	----	peaks	----	----	----	0.458	10	0.443	60	----	----	----	----
----	----	except	----	.414	1	----	----	----	----	.407	10	----	----
----	----	?-nuclepore	----	[4](.386	– 0.7)	----	----	.400	95	----	----	.3844	18
----	----	peak.	----	----	----	----	----	----	----	.324	2	----	----
----	----	----	----	.293	1	.304 to	Broad hump of	----	----	----	----	----	----
----	----	----	----	.276	1	.268	about 2.	----	----	----	----	.27185	100
0.259	10 M	----	----	.260	4	----	----	.259	20b	----	----	----	----
----	----	----	----	(.255	– 1)	----	----	----	----	.255	10	.25157	2
----	----	----	----	(.242	– 2)	----	----	.242	65	.244	7	----	----
----	----	----	----	.236	8	.238	Hint of	----	----	.234	6	.23540	11
----	----	----	----	----	----	----	a peak.	.233	70b	----	----	----	----
.225	10VS	----	----	(.217	– 1)	----	----	.221	10	----	----	----	----
----	----	----	----	.211	3	.210	Hint	.213	45	----	----	.21054	<1
----	----	----	----	(.206	– 1)	to	of a	.207	6	.206	4	----	----
----	----	----	----	.201	2	.201	hump.	----	----	----	----	.20069	9
----	----	----	----	.1915	7	.193	Hint	.190	14b	.1907	7	.19210	1
----	----	----	----	.188	1	to	of a	----	----	----	----	----	----
----	----	----	----	.185	1	.186	hump.	----	----	----	----	.18462	10
----	----	----	----	.1804	3	----	----	----	----	.1802	1	----	----
----	----	----	----	.176	.7	----	----	----	----	.1716	1	.17191	2
----	----	----	----	(.1675	– .7)	----	----	----	----	.1660	8	.16643	27
----	----	----	----	.1643	3	----	----	.1635	100	----	----	----	----
----	----	----	----	(.1623	– .7)	----	----	----	----	.1621	8	.16143	2
.158	7 S	----	----	.160	8	----	----	.1603	45b	----	----	----	----
----	----	----	----	.1532	1	----	----	----	----	.1541	3	.15272	2
----	----	----	----	.148	9	----	----	.1478	25bb	.1473	8	.14887	1

Table 6.—*Change in crystallinity with age and the correlation of electron diffraction patterns and a poorly defined X-ray diffraction pattern with published d_{hkl} values for nsutite, ramsdellite, and partridgeite—Continued.*

This work								Literature data					
Age, 3 hours				Age, 66 days				[1]γ-MnO_2 Nsutite		[2]MnO_2 Ramsdellite		[3]Mn_2O_3 Partridgeite	
Electron diffraction		X-ray diffraction		Electron diffraction		X-ray diffraction		X-ray diffraction		X-ray diffraction		X-ray diffraction	
d_{hkl} (nm)	I	d_{hkl} (nm)	I	d_{hkl} (nm)	I	d_{hkl} (nm)	I	d_{hkl} (nm)	I	d_{hkl} (nm)	I	d_{hkl} (nm)	I
----	----	----	----	.143	4	----	----	.1424	14	.1433	5	.14196	11
----	----	----	----	----	----	----	----	----	----	----	----	.13883	3
.135	6 W	----	----	.136	3	----	----	.1367	40bb	.1360	8	.13589	3
----	----	----	----	----	----	----	----	----	----	.1352	4	----	----
----	----	----	----	----	----	----	----	.1338	12b	.1337	1	----	----
----	----	----	----	.131	2	----	----	.1305	20bb	.1323	5	.13052	1
.129	6 M	----	----	.129	1	----	----	----	----	.1272	6	.12814	1
----	----	----	----	.1256	1	----	----	.1256	6	.1250	6	.12585	<1
----	----	----	----	.1226	5	----	----	.1210	10	.1219	3	----	----
----	----	----	----	.1185	4	----	----	.1168	6	----	----	.11772	1
----	----	----	----	----	----	----	----	----	----	----	----	.1755	1
----	----	----	----	----	----	----	----	----	----	----	----	.11591	1
----	----	----	----	----	----	----	----	----	----	----	----	.11579	1
----	----	----	----	.1123	1	----	----	----	----	----	----	.11252	1
.111	6 W	----	----	----	----	----	----	----	----	----	----	.11097	<1
----	----	----	----	----	----	----	----	----	----	----	----	.11087	<1
----	----	----	----	----	----	----	----	----	----	----	----	.10945	<1
----	----	----	----	.106	2	----	----	.1067	6	----	----	.10798	2
.100	7 W	----	----	.1003	1	----	----	.1043	6	----	----	----	----
----	----	----	----	.09716	2	----	----	----	----	----	----	----	----
----	----	----	----	.0953	3	----	----	----	----	----	----	----	----
----	----	----	----	.0938	.7	----	----	----	----	----	----	----	----
.0916	6 M	----	----	.0904	2	----	----	----	----	----	----	----	----

[1]Taken from Faulring (1965).
[2]Taken from Bystrom (1949).
[3]Taken from Swanson and others (1974).
[4](–) found in one view only.

Table 7.—*Change in crystallinity with age and the correlation of electron diffraction patterns and less well-defined X-ray diffraction patterns with published d_{hkl} values for β-MnOOH.*

[For electron diffraction, the number under intensity denotes the number of rings measured with that d_{hkl} to the most number of rings measured with a specific d_{hkl}. The actual intensity for electron diffraction patterns and for one X-ray diffraction pattern is listed in terms of W (weak), S (strong), and M (medium); for the other X-ray diffraction patterns, the intensities are numerically relative to the strongest peak.]

This work												Literature data			
Preparation 1								Preparation 2				[1]Pattern 1		[2]Pattern 2	
Age, 3 days				Age, 24 days				Age, 5 months							
Electron diffraction		X-ray diffraction		Electron diffraction		X-ray diffraction		Electron diffraction		X-ray diffraction		X-ray diffraction		X-ray diffraction	
d_{hkl} (nm)	I	d_{hkl} (nm)	I	d_{hkl} (nm)	I	d_{hkl} (nm)	I	d_{hkl} (nm)	I	d_{hkl} (nm)	I	d_{hkl} (nm)	I	d_{hkl} (nm)	I
0.462	6W	0.456	10	0.464	M	0.462	10	[3](0.465 –	W)	0.457	10	0.461	S	0.462	10
----	----	----	----	----	----	----	----	.281	W	----	----	----	----	----	----
----	----	----	----	----	----	----	----	Indistinct		.268	0.5	.267	M	.264	.5
.258	10S	.256	Hump	.256	S	.254	0.8	rings		.252	.3	----	----	----	----
Indistinct		to	of 2					between.							
rings			and												
between.		.242	less.												
.239	10M	----	----	.237	S	.237	.8	.237	M	.237	.4	.237	M	.236	broad 2
----	----	----	----	----	----	----	----	----	----	.229-?	.2	----	----	----	----
.196	2W	----	----	.197	W	.196	1	----	----	.196-?	.3	----	----	.196	broad 1
----	----	----	----	.185	W	.183	.5	.186	W	.184	.5	.184	M	----	----
----	----	----	----	----	----	----	----	.159	S	----	----	----	----	----	----
.157	10S	----	----	.157	S	----	----	Indistinct		.157-?	.3	.156	M	.155	----
Indistinct								rings							
rings								between.							
between.															
.149	10S	----	----	.150	S	----	----	----	----	----	----	.150	----	----	----
.145	3M	----	----	.145	M	----	----	.145	M	----	----	----	----	----	----
.1286	10M	----	----	.129M	to W	----	----	.1288	M	----	----	----	----	----	----
.1201	10M	----	----	.119	W	----	----	.1192	M	----	----	----	----	----	----
----	----	----	----	Many faint		----	----	.10525	W	----	----	----	----	----	----
----	----	----	----	rings beyond,		----	----	.0936	W	----	----	----	----	----	----
(.883 –	2W)	----	----	but too hard		----	----	Indistinct		----	----	----	----	----	----
				to define.				rings							
								between.							
(.853 –	2W)	----	----	--------		----	----	.0857	W	----	----	----	----	----	----

[1]Taken from Feitknecht and others (1962).
[2]Taken from Bricker (1965).
[3](–) found in one view only.

Figure 11.—View of platinum-shadowed, hexagonal- and lath-shaped platelets of β-MnOOH from preparation 2, aged 5 months. The magnification of this view is 1.6 times the magnification of the view of preparation 1 in figure 8.

Tables 3 through 7 list d_{hkl} values from electron diffraction patterns taken at 100 kV. Even if the R values were somewhat less than 4 mm, the results were as close to published d_{hkl} values as results obtained in this work from X-ray diffraction, where X-ray diffraction could be used. Examples are the 0.493 nm value in table 4 (corresponding to an R of 3.29 mm lengthwise of the film and of 3.35 mm across the film), the 0.472 nm value in table 6 (corresponding to an R of 3.43 mm lengthwise of the film and of 3.50 mm across the film), and the 0.46 nm values in table 7. So, with care, patterns of R's somewhat smaller than 4 mm can give satisfactory results and, as seen in table 6, patterns with R's substantially smaller can at least give indicative information.

Time and effort required

Another experimental limitation is the great amount of time and effort required to obtain the desired information. The sample preparation, the probable need for examining several views and mountings, the film development, and especially, the many radii measurements and the calculations and summaries of the corresponding d_{hkl}'s are all time consuming. However, for the identification of many microcrystalline solids that defy detection by X-ray, electron diffraction is an invaluable tool.

Other applications

Furthermore, besides being used for the study of manganese precipitates, the electron micrographs and electron diffraction methods discussed in this report have also been used in this laboratory for the identification of five other precipitates that were difficult to identify by X-ray alone. Some of these precipitates gave few or no X-ray patterns. The precipitates were from studies of: (1) the preparation of pure iron carbonate; (2) the preparation of iron oxides; (3) the conditions that favor the formation of bobierite and the conditions that favor the formation of fluorapatite; and (4) the identification of some natural aluminum sulfate sediments of spheroidal shape with a diameter of 0.1–0.2 μm. Some of these precipitates were obtained dried, and resuspension might possibly have altered their form and (or) their composition. The dried precipitates were, therefore, mounted by dusting the powder over the Formvar-covered grids.

CONCLUSIONS

Four manganese oxide minerals were identified by transmission electron microscope photography, by electron diffraction, and by X-ray diffraction. The data show that transmission electron microscopy and electron diffraction are valuable methods for identification of minerals that are too minute for identification by methods commonly used. Experimental data indicate that interpretation of electron diffraction patterns, as applied in this work, is as accurate as conventional X-ray diffraction results for d_{hkl}'s of 0.49 nm or less.

REFERENCES

Andrews, K. W., Dyson, D. J., and Keown, S. R., 1967, Interpretation of electron diffraction patterns: New York, Plenum Press, 188 p.

Beeston, B. E. P., Horne, R. W., and Markham, R., 1972, Electron diffraction and optical diffraction techniques, pt. 2, *in* Glauert, A. M., ed., Practical Methods in Electron Microscopy, v. 1: New York, Elsevier Publishing Company, 262 p.

Bricker, Owen, 1965, Some stability relations in the system $Mn\text{-}O_2\text{-}H_2O$ at 25° and one atmosphere total pressure: American Mineralogist, v. 50, p. 1296–1354.

Burns, R. G., and Burns, V. M., 1977, Mineralogy, *in* Glasby, G. P., ed., Marine Manganese Deposits: New York, Elsevier Scientific Publishing Company, 523 p.

Bystrom, A. M., 1949, Crystal structure of ramsdellite, an orthorhombic modification of manganese dioxide: Acta Chemica Scandinavica, v. 3, p. 163–173.

Faulring, G. M., 1965, Unit cell determinations and thermal transformations of nsutite: American Mineralogist, v. 50, p. 170–179.

Feitknecht, Walter, Brunner, P., and Oswald, H. R., 1962, Über den einfluss der feuchtigkeit auf die oxydation von

manganhydroxid durch molekularen sauerstoff: Zeitschrift für Anorganishe und Allgemeine Chemie, v. 316, p. 154–160.

Gattow, Gerhard, 1962, Definitions and characteristics of manganese oxides and hydroxides: Batterien, v. 16, p. 322–327.

Goodhew, P. J., 1972, Specimen preparation in material science, pt. 1, *in* Glauert, A. M., ed., Practical Methods in Electron Microscopy, v. 1: New York, Elsevier Publishing Company, 180 p.

Haine, M. E., and Cosslett, V. E., 1961, The electron microscope: London, E. and F. M. Spon Ltd., 282 p.

Hall, C. E., 1966, Introduction to electron microscopy [2d ed.]: New York, McGraw-Hill Book Company, 397 p.

Hem, J. D., 1980, Redox coprecipitation mechanisms of manganese oxide, *in* Kavanaugh, M. C., and Leckie, J. O., eds., Particulates in Water: Washington, D.C., American Chemical Society, American Chemical Society Advances in Chemistry Series, No. 189, p. 45–72.

Kay, D. H., ed., 1965, Techniques for electron microscopy [2d ed.]: Philadelphia, F. A. Davis Company, 560 p.

Klug, H. P., and Alexander, L. E., 1974, X-ray diffraction procedures for polycrystalline and amorphous materials: New York, John Wiley, 716 p.

Ross, Malcolm, 1959, Mineralogical applications of electron diffraction. II. Studies of some vanadium minerals of the Colorado Plateau: American Mineralogist, v. 44, p. 322–341.

Ross, Malcolm, and Christ, C. L., 1958, Mineralogical applications of electron diffraction. I. Theory and Techniques: American Mineralogist, v. 43, p. 1157–1178.

Rymer, T. B., 1970, Electron diffraction: London, Methuen and Company, 165 p.

Smith, J. V., ed., Berry, L. G., Post, Benjamin, and Weissmann, Sigmund, associate editors, Cohen, G. E., Bibliography, 1960, X-Ray powder data file sets 1–5 (Revised): Philadelphia, American Society for Testing Materials, 685 p.

Swanson, H. E., McMurdie, H. F., Morris, M. C., Evans, E. H., and Paretzkin, Boris, 1974, Standard X-ray diffraction powder patterns, Section 11—Data for 70 substances: *in* N.B.S. Monograph 25, p. 95.

Zwicker, W. K., Meijer, W. O. J. G., and Jaffee, H. W., 1962, Nsutite—a widespread manganese oxide mineral: American Mineralogist, v. 47, p. 246–266.